

# Dynamically generated resonances from the vector octet-baryon decuplet interaction

Sourav Sarkar<sup>1,2</sup>, Bao-Xi Sun<sup>1,3</sup>, E. Oset<sup>1</sup> and M.J. Vicente Vacas<sup>1</sup>

October 19, 2019

<sup>1</sup> Departamento de Física Teórica and IFIC, Centro Mixto Universidad de Valencia-CSIC, Institutos de Investigación de Paterna, Aptdo. 22085, 46071 Valencia, Spain

<sup>2</sup> Variable Energy Cyclotron Centre, 1/AF, Bidhannagar, Kolkata 700064, India

<sup>3</sup> Institute of Theoretical Physics, College of Applied Sciences, Beijing University of Technology, Beijing 100124, China

## Abstract

We study the interaction of the octet of vector mesons with the decuplet of baryons using Lagrangians of the hidden gauge theory for vector interactions. The unitary amplitudes in coupled channels develop poles that can be associated with some known baryonic resonances, while there are predictions for new ones at the energy frontier of the experimental research. The work offers guidelines on how to search for these resonances.

## 1 Introduction

The combination of chiral Lagrangians with nonperturbative unitary techniques in coupled channels has been very fruitful and has provided a powerful tool to study meson meson and meson baryon interactions beyond the realm of applicability of chiral perturbation theory. It leads to accurate cross sections for meson meson and meson baryon interactions and allows one to study the analytical properties of the scattering matrix, where poles are sometimes found, which can be associated to known resonances or new ones. Examples of this are the low lying scalar states found in the case of meson meson interaction [1, 2, 3, 4], the  $J^P = 1/2^-$  low lying baryon states found in the interaction of pseudoscalar mesons with baryons of the octet of the  $p$  [5, 6, 7, 8, 9, 10, 11, 12, 13, 14], and the  $J^P = 3/2^-$  states obtained from the interaction of pseudoscalar mesons with the decuplet of baryons of the  $\Delta$  [15, 16]. As an example of new states predicted, one has a second  $\Lambda(1405)$  state [17], right now reconfirmed by all the chiral unitary calculations, and which finds experimental support from the analysis of the  $K^-p \rightarrow \pi^0\pi^0\Sigma^0$  reaction [18] done in [19]. It also finds an

explanation for the new COSY data on  $\Lambda(1405)$  production in  $pp$  collisions [20] as shown in [21].

The work with vector mesons was for some time limited to the study of their interaction with pseudoscalar mesons, which generates the low lying axial vector mesons [22, 23] and a second  $K_1(1270)$  state [23], for which experimental evidence is found in [24].

A qualitative step in the interaction of vector mesons and generation of resonances was done in [25], where by using the Lagrangians of the hidden gauge approach to vector interactions [26, 27], one scalar and a tensor meson were found from the  $\rho\rho$  interactions, which could be identified with the  $f_0(1370)$  and  $f_2(1270)$  mesons, and for which the partial decay width into the sensitive  $\gamma\gamma$  decay channel was found to agree with experiment [28]. An extension to the full interaction of the octet of vector mesons among themselves has been recently done [29], indicating that several scalar, axial vectors and tensor states reported in the PDG [30] qualify as dynamically generated states from the vector-vector interaction.

In the baryon sector the interaction of vector mesons with baryons leading to generation of resonances was first done in [31] for the case of the  $\rho\Delta$  interaction, which leads to three  $N^*$  and three  $\Delta^*$  states in the vicinity of 1900 MeV, which are degenerate in  $J^P = 1/2^-, 3/2^-, 5/2^-$  within the approximations done, and which can be associated to existing states of the PDG.

After the successful predictions for the lowest states generated with vector mesons and baryons of the decuplet with  $\rho\Delta$ , the extension to the full  $SU(3)$  space of vectors and members of the decuplet of baryons is most opportune and this is the purpose of the present work. We extend the work of [31], using the formalism developed there, and we find *ten* states dynamically generated, some of which can be clearly associated to known resonances, while others are less clear. The states found are also degenerate in spin, and in some cases the known states of the PDG support this finding. In other cases one or two of these spin states are found in the PDG but others are missing. The findings of the present work indicate that such spin partners should exist and this offers a new motivation for the search of new baryonic resonances with the quantum numbers predicted.

## 2 Formalism for $VV$ interaction

We follow the formalism of the hidden gauge interaction for vector mesons of [26, 27] (see also [32] for a practical set of Feynman rules). The Lagrangian involving the interaction of vector mesons amongst themselves is given by

$$\mathcal{L}_{III} = -\frac{1}{4}\langle V_{\mu\nu}V^{\mu\nu} \rangle , \quad (1)$$

where the symbol  $\langle \rangle$  stands for the trace in the  $SU(3)$  space and  $V_{\mu\nu}$  is given by

$$V_{\mu\nu} = \partial_\mu V_\nu - \partial_\nu V_\mu - ig[V_\mu, V_\nu] , \quad (2)$$

where  $g$  is given by

$$g = \frac{M_V}{2f} , \quad (3)$$

with  $f = 93 \text{ MeV}$  the pion decay constant.  $V_\mu$  corresponds to the  $SU(3)$  matrix of the vectors of the octet of the  $\rho$  with the mixing of  $\phi$  and  $\omega$  accounted for and is given by

$$V_\mu = \begin{pmatrix} \frac{\rho^0}{\sqrt{2}} + \frac{\omega}{\sqrt{2}} & \rho^+ & K^{*+} \\ \rho^- & -\frac{\rho^0}{\sqrt{2}} + \frac{\omega}{\sqrt{2}} & K^{*0} \\ K^{*-} & \bar{K}^{*0} & \phi \end{pmatrix}_\mu . \quad (4)$$

The interaction of  $\mathcal{L}_{III}$  gives rise to a three vector vertex form

$$\mathcal{L}_{III}^{(3V)} = ig \langle (\partial_\mu V_\nu - \partial_\nu V_\mu) V^\mu V^\nu \rangle , \quad (5)$$

which can be conveniently rewritten using the property of the trace as

$$\mathcal{L}_{III}^{(3V)} = ig \langle [V^\mu (\partial_\nu V_\mu) - (\partial_\nu V_\mu) V^\mu] V^\nu \rangle . \quad (6)$$

With the three vector coupling we can construct the Feynman diagram which is responsible for the vector baryon decuplet interaction through the exchange of a vector between two vectors and the baryon, see fig. 1(b), in analogy with the interaction of a pseudoscalar meson with the baryon decuplet depicted in fig. 1(a). This mechanism of interaction of pseudoscalars with baryons, leads to the well known Weinberg-Tomozawa term, upon neglecting  $q^2/M_V^2$  in the propagator of the exchanged vector, where  $q$  is the momentum transfer. The local chiral Lagrangian for vector baryon decuplet interaction can thus be obtained from this formalism upon neglecting the momentum transfer compared to the mass of the vector, a good approximation for the purpose of studying the interaction relatively close to threshold where bound states or resonances are searched for. Consistent with this implicit approximation of the chiral Lagrangians, we neglect the three-momentum of the vectors compared to their mass. In this approximation the polarization vectors of the vector mesons have only spatial components. This simplifies considerably the formalism. Indeed, let us look at eq. (6) where we see that the field  $V^\nu$  cannot correspond to an external vector meson. Indeed, if this were the case, the  $\nu$  index should be spatial and then the partial derivative  $\partial_\nu$  would lead to a three momentum of the vector mesons which are neglected in the approach. Then  $V^\nu$  corresponds to the exchanged vector. In this case one finds an analogy to the coupling of vectors to pseudoscalars given in the same theory by

$$\mathcal{L}_{VPP} = -ig \langle [P(\partial_\nu P) - (\partial_\nu P)P] V^\nu \rangle , \quad (7)$$

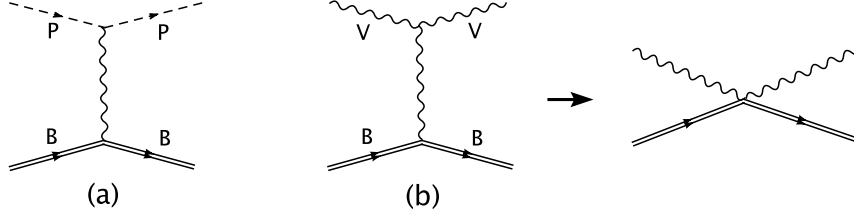


Figure 1: Diagrams contributing to the pseudoscalar-baryon (a) or vector- baryon (b) interaction via the exchange of a vector meson leading to the effective vector-baryon contact interaction which is used in the Bethe-Salpeter equation

where  $P$  is the  $SU(3)$  matrix of the pseudoscalar fields. The only difference is the polarization vector of the two external fields and a sign, which recalling that we only have spatial components for the external vectors, results in the factor  $\vec{\epsilon} \cdot \vec{\epsilon}'$  additional to the contribution from the  $PPV$  Lagrangian of eq. (7), from the upper vertex of fig. 1 (a).

Consequently, in order to obtain the tree level amplitudes corresponding to the diagram of fig. 1(b), all one has to do is to take the corresponding amplitudes of pseudoscalar meson-baryon decuplet interaction, substituting the  $SU(3)$  pseudoscalar matrix by the corresponding one of the vector mesons. That is,  $\pi^+ \Delta^+ \rightarrow \pi^+ \Delta^+$  is substituted by  $\rho^+ \Delta^+ \rightarrow \rho^+ \Delta^+$  and so on.

A small amendment is in order, which is due to the mixing of  $\omega_8$  and the singlet of  $SU(3)$ ,  $\omega_1$ , to give the physical states of  $\omega$  and  $\phi$

$$\begin{aligned}\omega &= \frac{2}{\sqrt{6}}\omega_1 + \frac{1}{\sqrt{3}}\omega_8 \\ \phi &= \frac{1}{\sqrt{3}}\omega_1 - \frac{2}{\sqrt{6}}\omega_8\end{aligned}\tag{8}$$

Given the structure of eq. (8), the singlet state which is accounted for by the  $V$  matrix,  $diag(\omega_1, \omega_1, \omega_1)/\sqrt{3}$ , does not provide any contribution to eq. (6), in which case, one simply has to take the matrix elements known for the  $PB$  interaction and wherever  $P$  is the  $\eta_8$  multiply the amplitude by the factor  $1/\sqrt{3}$  to get the corresponding  $\omega$  contribution and by  $-\sqrt{2/3}$  to get the corresponding  $\phi$  contribution.

We take the matrix elements for the amplitudes from [16]. There the same approximations that we make for the vector mesons, neglecting the the three-momentum versus their mass, were also done for the baryons and then all the amplitudes have the form

$$V_{ij} = -C_{ij} \frac{1}{4f^2} (k^0 + k'^0) \vec{\epsilon} \cdot \vec{\epsilon}',\tag{9}$$

where  $k^0, k'^0$  are the energies of the incoming and outgoing vector meson respectively. The amplitudes are thus exactly the ones for  $PB \rightarrow PB$  apart for the factor  $\vec{\epsilon} \cdot \vec{\epsilon}'$ .

The  $C_{ij}$  coefficients of eq. (9) can be obtained directly from [16] with the simple rules given above for the  $\omega$  and the  $\phi$ , and substituting  $\pi$  by  $\rho$  and  $K$  by  $K^*$  in the matrix elements. The coefficients are obtained both in the physical basis of states and in the isospin basis. Here we will directly study the interaction in isospin basis and we collect the tables of the  $C_{ij}$  coefficients in the Appendix for different states of isospin,  $I$ , and strangeness,  $S$ .

Inspection of the tables immediately show the cases where we find attractive interaction and we can expect bound states or resonances, and where there is repulsion no states should be expected. We find attraction in the channels  $S, I = 0, 1/2; 0, 3/2; -1, 0; -1, 1; -2, 1/2$  and maybe  $-3, 0$ , where the diagonal terms are zero but one can get bound states through the interplay of the nondiagonal terms of the coupled channels. On the other hand in the  $0, 5/2; -1, 2; -2, 3/2; -3, 1$  and  $-4, 1/2$  one finds repulsion and one should not expect bound states or resonances there. Interestingly, these are all exotic channels and we find that even if these exotic quantum numbers can be reached within the approach, for dynamical reasons, no bound states are found in either of the possible exotic channels.

The next step to construct the scattering matrix is done by solving the coupled channels Bethe Salpeter equation in the on shell factorization approach of [8, 9]

$$T = [1 - V G]^{-1} V \quad (10)$$

with  $G$  the loop function of a vector meson and a baryon which we calculate in dimensional regularization using the formula of [9], with  $\mu$  a regularization scale of 700 MeV, and natural values of the subtraction constants  $a_l(\mu)$  around -2, as determined in [9].

The iteration of diagrams implicit in the Bethe Salpeter equation in the case of the vector mesons has a subtlety with respect to the case of the pseudoscalars. The  $\vec{\epsilon} \cdot \vec{\epsilon}'$  term of the interaction forces the intermediate vector mesons in the loops to propagate with the spatial components in the loops. We need to sum over the polarizations of the internal vector mesons which, because they are tied to the external ones through the  $\vec{\epsilon} \cdot \vec{\epsilon}'$  factor, provides

$$\sum_{pol} \epsilon_i \epsilon_j = \delta_{ij} + \frac{q_i q_j}{M_V^2} \quad (11)$$

As shown in [23], the on shell factorization leads to a correction coefficient in the  $G$  function of  $\vec{q}^2/3M_V^2$  versus unity, which is negligibly small, and is also neglected here for consistency with the approximations done. In this case the factor  $\vec{\epsilon} \cdot \vec{\epsilon}'$  appearing in the potential  $V$ , factorizes also in the  $T$  matrix for the external vector mesons.

Since the spin dependence only comes from the  $\vec{\epsilon} \cdot \vec{\epsilon}'$  factor and there is no dependence on the spin of the baryons, the interaction for vector-baryon states with  $1/2^-, 3/2^-$  and  $5/2^-$  is the same and thus we get three degenerate states for each of the resonances found. The spin degeneracy also appears in some quark models [33].

Finally, as done in [31], we take into account the convolution of the  $G$  function with the mass distributions of the  $\rho$ ,  $K^*$ ,  $\Delta$ ,  $\Sigma(1385)$  and  $\Xi(1530)$  states, in order to account for their sizeable width.

### 3 Results

In this section we show results for the amplitudes obtained in the attractive channels mentioned above. In figs 2,3,4 we show the results for the channels  $S, I = 0, 1/2; 0, 3/2; -1, 0; -1, 1; -2, 1/2$  and  $-3, 0$ . The value of  $a_l(\mu)$  taken is  $-2.2$  MeV.

#### 3.1 $S, I=0, 1/2$ states

The figures show peaks of  $|T|^2$  which indicate the existence of a pole or a resonance. To further verify the guess, we look for poles in the complex plane as done in [8, 9, 23]. The real part of the pole position provides the mass of the resonance and two times the imaginary part its width. The results can be seen in tables 11, 12, 13, 14, 15, 16. In fig. 2 we show the results for the  $S, I = 0, 1/2; 0, 3/2$  channels. In the  $S, I = 0, 1/2$  sector (fig. 2(left)) we see a clear peak around 1850 MeV, most pronounced in the  $\Delta\rho$  channel, but also visible in  $\Sigma^*K^*$ . This is also reflected in the couplings in table 11. This difference in the couplings and the large mass difference of the  $\Sigma^*K^*$  state with respect to the mass of the resonance makes the effect of this channel essentially negligible and the state qualifies cleanly as a  $\Delta\rho$  state, as was assumed in [31]. The second weak structure around 2270 MeV on the  $\Sigma^*K^*$  threshold does not correspond to a pole. Note, however, that such a bump could be identified experimentally with a resonance. In fact, there is a catalogued resonance  $N^*(2200)(5/2^-)$  around that energy.

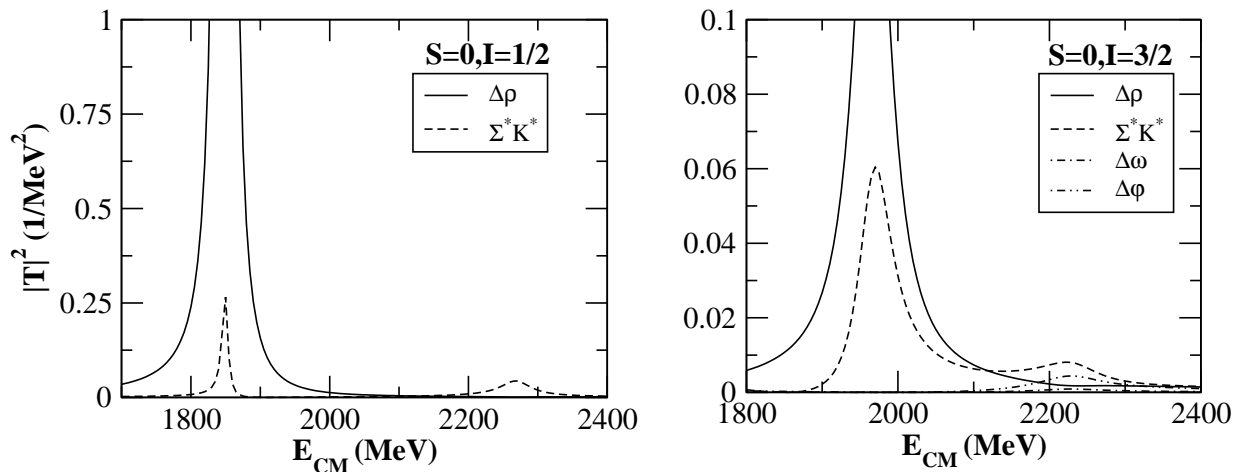


Figure 2:  $|T|^2$  for  $S, I = 0, 1/2$  and  $0, 3/2$ .

#### 3.2 $S, I=0, 3/2$ states

In this case we see a clear peak in fig. 2(right) that shows mostly in the  $\Delta\rho$  channel. An inspection of table 12 also indicates substantial coupling to the  $\Sigma^*K^*$  channel. This state was obtained in [31] considering only the  $\Delta\rho$  channel. A posteriori, we corroborate the

approach of [31] which was justified there in the fact that the lowest mass states should be constructed with the lowest mass vector and meson. The channel  $\Delta\omega$  which has about the same mass as that of the  $\Delta\rho$  was ignored in [31] since, as one can see in table 3, it does not couple to the  $\Delta\rho$  nor to itself. Now the final coupling of the  $\Delta\omega$  to the resonance is not zero, although negligible. The reason is that the coupled channel treatment allows this resonance to couple to  $\Delta\omega$  through nondiagonal transitions to the  $\Sigma^*K^*$  state. The weaker broad structure that appears around 2200 MeV in the  $\Sigma^*K^*$  channel does not correspond to a pole in the complex plane. However, we should note that with a slightly weaker subtraction constant,  $a = -2.1$ , it shows much more neatly and around 2150 MeV, and could be associated with the catalogued  $\Delta(2150)(1/2^-)$ .

### 3.3 $S, I = -1, 0$ states

In fig. 3(left) we find a clear peak around 2050 MeV which is most visible in the  $\Sigma^*\rho$  channel but also couples to the  $\Xi^*K^*$ . This is corroborated by the strength of the couplings in table 13. There is a weaker structure in the  $\Xi^*K^*$  channel around 2400 MeV (at threshold) which does not correspond to a pole in the complex plane.

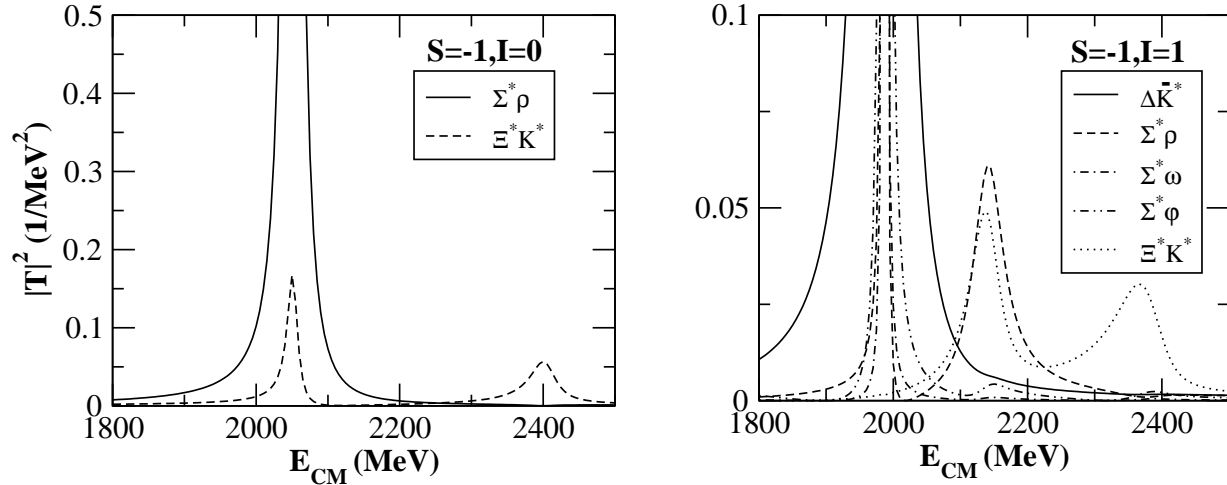


Figure 3:  $|T|^2$  for  $S, I = -1, 0$  and  $-1, 1$ .

### 3.4 $S, I = -1, 1$ states

Fig 3(right) shows this case where there are five coupled channels producing three structures in the amplitude squared which indeed correspond to three poles as shown in table 14. The first around 1950 MeV couples strongly to  $\Delta\bar{K}^*$ , another one near 2150 MeV that couples strongly to  $\Sigma^*\rho$  and  $\Xi^*K^*$ , and a third broader one around 2380 MeV that couples mostly to  $\Xi^*K^*$ .

### 3.5 $S, I = -2, 1/2$ states

In this case also there are five coupled channels. One finds three clear structures in fig 4(left) which correspond to three poles of the scattering amplitude. The one around 2200 MeV couples mostly to  $\Sigma^* \bar{K}^*$  and  $\Xi^* \phi$  as seen from table 15. The second, around 2300 MeV is seen prominently in the  $\Xi^* \rho$  channel. The other around 2520 MeV couples mostly to  $\Omega K^*$  and appears as a distinct peak structure in this channel.

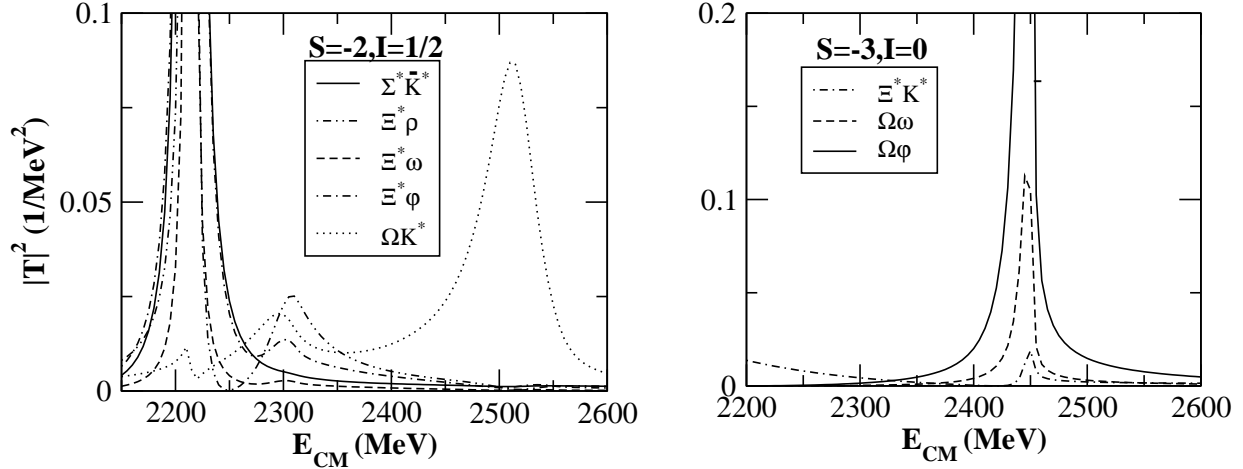


Figure 4:  $|T|^2$  for  $S, I = -2, 1/2$  and  $-3, 0$ .

### 3.6 $S, I = -3, 0$ states

We see in fig. 4(right) a clear peak around 2450 MeV corresponding to a pole in the complex energy plane around this energy. As seen from table 16, this state couples mostly to  $\Omega \phi$  and  $\Omega \omega$ .

## 4 Comparison to data

It is interesting to compare with data of the PDG. A summary is presented in table 1 in which the 10 dynamically generated states have been listed along with their possible PDG counterparts including their present status and properties. The two states that we find for  $S, I = 0, 1/2$  and  $0, 3/2$  around 1850 MeV and 1970 MeV respectively were discussed in detail in [31]. We do not discuss them further but recall that there are indeed natural candidates for these states in the  $\Delta(1900) \ 3/2(1/2^-)$ ,  $\Delta(1940) \ 3/2(3/2^-)$   $\Delta(1930) \ 3/2(5/2^-)$ . As discussed there, some fine tuning of the subtraction constant can make the masses agree better. But differences of 50 MeV or more are the state of the art in determining masses in hadronic models. As to the  $N^*$  states around these energies, we mention, recalling [31] that there is a large dispersion of data in the masses but there are indeed several candidate



$S, I$	Theory			PDG data				
	pole position	real axis		name	$J^P$	status	mass	width
		mass	width					
0, 1/2	$1850 + i5$	1850	11	$N(2090)$	$1/2^-$	★	1880-2180	95-414
				$N(2080)$	$3/2^-$	★★	1804-2081	180-450
		$2270(bump)$		$N(2200)$	$5/2^-$	★★	1900-2228	130-400
0, 3/2	$1972 + i49$	1971	52	$\Delta(1900)$	$1/2^-$	★★	1850-1950	140-240
				$\Delta(1940)$	$3/2^-$	★	1940-2057	198-460
				$\Delta(1930)$	$5/2^-$	★★★	1900-2020	220-500
		$2200(bump)$		$\Delta(2150)$	$1/2^-$	★	2050-2200	120-200
-1, 0	$2052 + i10$	2050	19	$\Lambda(2000)$	$?^?$	★	1935-2030	73-180
-1, 1	$1987 + i1$	1985	10	$\Sigma(1940)$	$3/2^-$	★★★	1900-1950	150-300
	$2145 + i58$	2144	57	$\Sigma(2000)$	$1/2^-$	★	1944-2004	116-413
	$2383 + i73$	2370	99	$\Sigma(2250)$	$?^?$	★★★	2210-2280	60-150
				$\Sigma(2455)$	$?^?$	★★	$2455 \pm 10$	100-140
-2, 1/2	$2214 + i4$	2215	9	$\Xi(2250)$	$?^?$	★★	2189-2295	30-130
	$2305 + i66$	2308	66	$\Xi(2370)$	$?^?$	★★	2356-2392	75-80
	$2522 + i38$	2512	60	$\Xi(2500)$	$?^?$	★	2430-2505	59-150
-3, 1	$2449 + i7$	2445	13	$\Omega(2470)$	$?^?$	★★	$2474 \pm 12$	$72 \pm 33$

Table 1: The properties of the 10 dynamically generated resonances and their possible PDG counterparts. We also include the  $N^*$  bump around 2270 MeV and the  $\Delta^*$  bump around 2200 MeV.

states like the  $N^*(2090)$   $1/2(1/2^-)$ ,  $N^*(2080)$   $1/2(3/2^-)$  etc. though some of the states predicted could be missing.

The  $\Lambda^*$  state that we see in  $S, I = -1, 0$  around 2050 MeV could correspond to the  $\Lambda(2000)$  with spin parity unknown. We do not see traces of the spin partners in this energy region.

In the  $\Sigma^*$  sector we found three states around 1990, 2150, 2380 MeV. One can find two states around 2000 MeV in table 1,  $\Sigma(1940)$  ( $3/2^-$ ) and  $\Sigma(2000)$  ( $1/2^-$ ). At higher energies there are several states. One of them, the  $\Sigma^*(2250)$  classified with three stars, where some

experiments see two resonances, one of them with  $5/2^-$ . Another one is the  $\Sigma^*(2455)$  classified as bumps without spin and parity assignment. This region is the experimental frontier in this sector and we hope that the findings of the present work stimulate further work to complete the table. Indeed, the information we provide, telling to which states the resonance couples most strongly could be a guiding line for the search of these new states.

In the  $\Xi^*$ ,  $S, I = -2, 1/2$  sector we find three states around 2200 MeV, 2300 MeV and 2520 MeV. As shown in table 1 in the PDG, we find three states  $\Xi(2250)$ ,  $\Xi(2370)$ ,  $\Xi(2500)$  with spin and parity unknown. This sector is also poorly known but an experimental program is running at Jefferson Lab to widen the information in this sector [34, 35].

Finally, in the  $\Omega$  sector we find a clean state around 2450 MeV. Once again we find in the PDG the  $\Omega(2470)$  without spin and parity assigned.

The width of the resonances in the present framework is given by twice the imaginary part of the pole position in the complex energy plane. Also reported in the 'real-axis' column of table 1 is the full width at half maximum obtained from the square of the amplitude plotted as a function of energy. However, we do not consider it meaningful to compare the widths of the dynamically generated states with those of the PDG in this work. Those reported here correspond only to decay into the vector-baryon decuplet states. In addition there are decays into a pseudoscalar meson and an octet baryon which can also be calculated in this approach, in a similar way as it was done in [25] to obtain the decay into  $\pi\pi$  of the  $\rho\rho$  states found there. Given the incomplete information about the states in the PDG in this area and the qualitative assignments that we can only do at present, its evaluation would not provide more help establishing the association of theoretical states with the experimental ones, but when the situation improves, this work could be done to help understand better the spectrum of baryons.

## 5 Conclusions

We have studied the interaction of vector mesons with the decuplet of baryons, looking for bound states or resonances, and we find ten poles in the scattering matrices of different strangeness and isospin channels. The states are furthermore degenerate in  $J^P = 1/2^-, 3/2^-, 5/2^-$ . We found candidates in the PDG to be associated to the states found, but many of them are missing. This should not be a surprise since the states we find are at the frontier of the experimental research. The success of the method applied in other sectors, as the meson sector, and even here for the lowest energy states found, makes us confident that these states exist. The difficulties in finding them are understandable. Most of the states reported in this energy region are found in partial wave analysis of reactions using the available pion, photon, electron or kaon beams. Some of these analyses require the simultaneous consideration of many resonances, more than twenty in some cases, which makes the conclusions problematic. Indeed, different solutions are often found, concerning not only the properties but even the existence of some resonances, depending on the type of analysis or the assumptions made. New schemes become necessary to make progress in this area. In this sense, the present theoretical work, as well as others, where predictions

are made regarding the channels to which the resonances couple most strongly, could be considered as a guideline to search for specific final states which could filter some of the resonances. We envisage a fruitful new strategy of research along this line and encourage future work in this direction.

## Acknowledgments

B. X. Sun would like to thank Li-Sheng Geng and R. Molina for useful discussions. This work is partly supported by DGICYT contract number FIS2006-03438. This research is part of the EU Integrated Infrastructure Initiative Hadron Physics Project under contract number RII3-CT-2004-506078. B. X. Sun acknowledges support from the National Natural Science Foundation of China under grant number 10775012.

## References

- [1] J. A. Oller and E. Oset, Nucl. Phys. A **620**, 438 (1997) [Erratum-ibid. A **652**, 407 (1999)] [arXiv:hep-ph/9702314].
- [2] J. A. Oller, E. Oset and J. R. Pelaez, Phys. Rev. D **59**, 074001 (1999) [Erratum-ibid. D **60**, 099906 (1999 ERRAT,D75,099903.2007)] [arXiv:hep-ph/9804209].
- [3] N. Kaiser, Eur. Phys. J. A **3**, 307 (1998).
- [4] V. E. Markushin, Eur. Phys. J. A **8**, 389 (2000) [arXiv:hep-ph/0005164].
- [5] N. Kaiser, P. B. Siegel and W. Weise, Phys. Lett. B **362**, 23 (1995) [arXiv:nucl-th/9507036].
- [6] N. Kaiser, P. B. Siegel and W. Weise, Nucl. Phys. A **594**, 325 (1995) [arXiv:nucl-th/9505043].
- [7] N. Kaiser, T. Waas and W. Weise, Nucl. Phys. A **612**, 297 (1997) [arXiv:hep-ph/9607459].
- [8] E. Oset and A. Ramos, Nucl. Phys. A **635** (1998) 99 .
- [9] J. A. Oller and U. G. Meissner, Phys. Lett. B **500**, 263 (2001) [arXiv:hep-ph/0011146].
- [10] C. Garcia-Recio, M. F. M. Lutz and J. Nieves, Phys. Lett. B **582** (2004) 49 .
- [11] C. Garcia-Recio, J. Nieves and L. L. Salcedo, Phys. Rev. D **74** (2006) 034025 .
- [12] T. Hyodo, S. I. Nam, D. Jido and A. Hosaka, Phys. Rev. C **68**, 018201 (2003) [arXiv:nucl-th/0212026].

- [13] T. Hyodo, D. Jido and A. Hosaka, Phys. Rev. D **75**, 034002 (2007) [arXiv:hep-ph/0611004].
- [14] T. Inoue, E. Oset and M. J. Vicente Vacas, Phys. Rev. C **65**, 035204 (2002) [arXiv:hep-ph/0110333].
- [15] E. E. Kolomeitsev and M. F. M. Lutz, Phys. Lett. B **585** (2004) 243 .
- [16] S. Sarkar, E. Oset and M. J. Vicente Vacas, Nucl. Phys. A **750** (2005) 294 [Erratum-ibid. A **780** (2006) 78] .
- [17] D. Jido, J. A. Oller, E. Oset, A. Ramos and U. G. Meissner, Nucl. Phys. A **725**, 181 (2003) [arXiv:nucl-th/0303062].
- [18] S. Prakhov *et al.* [Crystall Ball Collaboration], Phys. Rev. C **70**, 034605 (2004).
- [19] V. K. Magas, E. Oset and A. Ramos, Phys. Rev. Lett. **95**, 052301 (2005) [arXiv:hep-ph/0503043].
- [20] I. Zychor *et al.*, Phys. Lett. B **660**, 167 (2008) [arXiv:0705.1039 [nucl-ex]].
- [21] L. S. Geng, E. Oset and M. Doring, Eur. Phys. J. A **32**, 201 (2007) [arXiv:hep-ph/0702093].
- [22] M. F. M. Lutz and E. E. Kolomeitsev, Nucl. Phys. A **730**, 392 (2004) [arXiv:nucl-th/0307039].
- [23] L. Roca, E. Oset and J. Singh, Phys. Rev. D **72**, 014002 (2005) [arXiv:hep-ph/0503273].
- [24] L. S. Geng, E. Oset, L. Roca and J. A. Oller, Phys. Rev. D **75**, 014017 (2007) [arXiv:hep-ph/0610217].
- [25] R. Molina, D. Nicmorus and E. Oset, arXiv:0809.2233 [hep-ph].
- [26] M. Bando, T. Kugo, S. Uehara, K. Yamawaki and T. Yanagida, Phys. Rev. Lett. **54**, 1215 (1985).
- [27] M. Bando, T. Kugo and K. Yamawaki, Phys. Rept. **164**, 217 (1988).
- [28] H. Nagahiro, J. Yamagata-Sekihara, E. Oset and S. Hirenzaki, arXiv:0809.3717 [hep-ph].
- [29] L. S. Geng and E. Oset, arXiv:0812.1199 [hep-ph].
- [30] C. Amsler *et al.* [Particle Data Group], Phys. Lett. B **667**, 1 (2008).
- [31] P. Gonzalez, E. Oset and J. Vijande, Phys. Rev. C in print, arXiv:0812.3368 [hep-ph].

- [32] H. Nagahiro, L. Roca, A. Hosaka and E. Oset, arXiv:0809.0943 [hep-ph].
- [33] M. Kirchbach and C. B. Compean, Eur. Phys. J. A 39, 1 (2007) arXiv:0805.2404 [hep-ph].
- [34] B. M. K. Nefkens, AIP Conf. Proc. **870**, 405 (2006).
- [35] J. W. Price *et al.* [CLAS Collaboration], Phys. Rev. C **71**, 058201 (2005) [arXiv:nucl-ex/0409030].

## 6 Appendix

	$\Delta\rho$	$\Sigma^*K^*$
$\Delta\rho$	5	2
$\Sigma^*K^*$		2

Table 2:  $C_{ij}$  coefficients for  $S = 0$ ,  $I = \frac{1}{2}$ .

	$\Delta\rho$	$\Sigma^*K^*$	$\Delta\omega$	$\Delta\phi$
$\Delta\rho$	2	$\sqrt{\frac{5}{2}}$	0	0
$\Sigma^*K^*$		-1	$\sqrt{\frac{3}{2}}$	$-\sqrt{3}$
$\Delta\omega$			0	0
$\Delta\phi$				0

Table 3:  $C_{ij}$  coefficients for  $S = 0$ ,  $I = \frac{3}{2}$ .

	$\Sigma^*\rho$	$\Xi^*K^*$
$\Sigma^*\rho$	4	$\sqrt{6}$
$\Xi^*K^*$		3

Table 4:  $C_{ij}$  coefficients for  $S = -1$ ,  $I = 0$ .

	$\Delta\overline{K}^*$	$\Sigma^*\rho$	$\Sigma^*\omega$	$\Sigma^*\phi$	$\Xi^*K^*$
$\Delta\overline{K}^*$	4	1	$\sqrt{2}$	-2	0
$\Sigma^*\rho$		2	0	0	2
$\Sigma^*\omega$			0	0	$\sqrt{2}$
$\Sigma^*\phi$				0	-2
$\Xi^*K^*$					1

Table 5:  $C_{ij}$  coefficients for  $S = -1$ ,  $I = 1$ .

	$\Delta\overline{K}^*$	$\Sigma^*\rho$
$\Delta\overline{K}^*$	0	$\sqrt{3}$
$\Sigma^*\rho$		-2

Table 6:  $C_{ij}$  coefficients for  $S = -1$ ,  $I = 2$ .

	$\Sigma^*\overline{K}^*$	$\Xi^*\rho$	$\Xi^*\omega$	$\Xi^*\phi$	$\Omega K^*$
$\Sigma^*\overline{K}^*$	2	1	$\sqrt{3}$	$-\sqrt{6}$	0
$\Xi^*\rho$		2	0	0	$\frac{3}{\sqrt{2}}$
$\Xi^*\omega$			0	0	$\sqrt{\frac{3}{2}}$
$\Xi^*\phi$				0	$-\sqrt{3}$
$\Omega K^*$					3

Table 7:  $C_{ij}$  coefficients for  $S = -2$ ,  $I = \frac{1}{2}$ .

	$\Sigma^*\overline{K}^*$	$\Xi^*\rho$
$\Sigma^*\overline{K}^*$	-1	2
$\Xi^*\rho$		-1

Table 8:  $C_{ij}$  coefficients for  $S = -2$ ,  $I = \frac{3}{2}$ .

	$\Xi^* \bar{K}^*$	$\Omega\omega$	$\Omega\phi$
$\Xi^* \bar{K}^*$	0	$\sqrt{3}$	$-\sqrt{6}$
$\Omega\omega$		0	0
$\Omega\phi$			0

Table 9:  $C_{ij}$  coefficients for  $S = -3$ ,  $I = 0$ .

	$\Xi^* \bar{K}^*$	$\Omega\rho$
$\Xi^* \bar{K}^*$	-2	$\sqrt{3}$
$\Omega\rho$		-2

Table 10:  $C_{ij}$  coefficients for  $S = -3$ ,  $I = 1$ .

$z_R$	$1850 + i5$	
	$g_i$	$ g_i $
$\Delta\rho$	$4.9 + i0.1$	4.9
$\Sigma^* K^*$	$1.7 + i0.0$	1.7

Table 11: The position of the pole and the coupling constant  $g_i$  of the resonance for  $S = 0$ ,  $I = \frac{1}{2}$ .

$z_R$	$1972 + i49$	
	$g_i$	$ g_i $
$\Delta\rho$	$5.0 + i0.2$	5.0
$\Sigma^* K^*$	$3.9 - i0.1$	3.9
$\Delta\omega$	$-0.1 + i0.2$	0.3
$\Delta\phi$	$0.2 - i0.4$	0.4

Table 12: The position of the pole and the coupling constant  $g_i$  of the resonance for  $S = 0$ ,  $I = \frac{3}{2}$ .



$z_R$	2052 + $i$ 10	
	$g_i$	$ g_i $
$\Sigma^* \rho$	4.2 + $i$ 0.1	4.2
$\Xi^* K^*$	2.0 + $i$ 0.1	2.0

Table 13: The position of the pole and the coupling constant  $g_i$  of the resonance for  $S = -1$ ,  $I = 0$ .

$z_R$	1987 + $i$ 1		2145 + $i$ 58		2383 + $i$ 73	
	$g_i$	$ g_i $	$g_i$	$ g_i $	$g_i$	$ g_i $
$\Delta \overline{K}^*$	4.2 + $i$ 0.0	4.2	0.7 + $i$ 0.1	0.7	0.4 + $i$ 0.4	0.6
$\Sigma^* \rho$	1.4 + $i$ 0.0	1.4	-4.3 - $i$ 0.7	4.4	0.4 + $i$ 1.1	1.2
$\Sigma^* \omega$	1.4 + $i$ 0.0	1.4	1.3 - $i$ 0.4	1.3	-1.4 - $i$ 0.4	1.5
$\Sigma^* \phi$	-2.1 - $i$ 0.0	2.1	-1.9 + $i$ 0.6	2.0	2.1 + $i$ 0.6	2.2
$\Xi^* K^*$	0.1 - $i$ 0.0	0.1	-4.0 - $i$ 0.1	4.0	-3.5 + $i$ 1.5	3.8

Table 14: The position of the pole and the coupling constant  $g_i$  of the resonance for  $S = -1$ ,  $I = 1$ .

$z_R$	2214 + $i$ 4		2305 + $i$ 66		2522 + $i$ 38	
	$g_i$	$ g_i $	$g_i$	$ g_i $	$g_i$	$ g_i $
$\Sigma^* \overline{K}^*$	2.4 + $i$ 0.1	2.4	0.8 - $i$ 0.1	0.8	0.3 + $i$ 0.3	0.4
$\Xi^* \rho$	1.8 - $i$ 0.1	1.8	-3.5 - $i$ 1.7	3.9	0.2 + $i$ 1.0	1.0
$\Xi^* \omega$	1.7 + $i$ 0.1	1.7	2.0 - $i$ 0.7	2.1	-0.6 - $i$ 0.3	0.7
$\Xi^* \phi$	-2.5 - $i$ 0.1	2.5	-3.0 + $i$ 1.0	3.1	0.9 + $i$ 0.4	1.0
$\Omega K^*$	0.5 - $i$ 0.1	0.5	-2.7 - $i$ 0.8	2.8	-3.3 + $i$ 0.9	3.4

Table 15: The position of the pole and the coupling constant  $g_i$  of the resonance for  $S = -2$ ,  $I = 1/2$ .

$z_R$	$2449 + i7$	
	$g_i$	$ g_i $
$\Xi^* \overline{K}^*$	$1.0 + i0.2$	1.0
$\Omega\omega$	$1.6 - i0.2$	1.7
$\Omega\phi$	$-2.4 + i0.3$	2.5

Table 16: The position of the pole and the coupling constant  $g_i$  of the resonance for  $S = -3$ ,  $I = 0$ .